

Environmental Regulation of Lateral Root Emergence in *Medicago truncatula* Requires the HD-Zip I Transcription Factor HB1 ^W

Federico Ariel,^{a,1} Anouck Diet,^{b,c,1} Marion Verdenaud,^d Véronique Gruber,^{b,c,1} Florian Frugier,^b Raquel Chan,^a and Martin Crespi^{b,2}

^aInstituto de Agrobiotecnología del Litoral, Consejo Nacional de Investigaciones Científicas y Técnicas, Universidad Nacional del Litoral, CP 3000 Santa Fe, Argentina

^bInstitut des Sciences du Végétal, Centre National de la Recherche Scientifique, F91198 Gif sur Yvette, France

^cUniversité Paris Diderot Paris 7, Les Grands Moulins, F-75205 Paris Cedex 13, France

^dLaboratoire des Interactions Plantes Micro-organismes, Centre National de la Recherche Scientifique, Institut National de la Recherche Agronomique, 31326 Castanet-Tolosan, France

The adaptation of root architecture to environmental constraints is a major agricultural trait, notably in legumes, the third main crop worldwide. This root developmental plasticity depends on the formation of lateral roots (LRs) emerging from primary roots. In the model legume *Medicago truncatula*, the HD-Zip I transcription factor HB1 is expressed in primary and lateral root meristems and induced by salt stress. Constitutive expression of HB1 in *M. truncatula* roots alters their architecture, whereas *hb1* TILLING mutants showed increased lateral root emergence. Electrophoretic mobility shift assay, promoter mutagenesis, and chromatin immunoprecipitation–PCR assays revealed that HB1 directly recognizes a CAA-TAATTG cis-element present in the promoter of a LOB-like (for Lateral Organ Boundaries) gene, *LBD1*, transcriptionally regulated by auxin. Expression of these genes in response to abscisic acid and auxin and their behavior in *hb1* mutants revealed an HB1-mediated repression of *LBD1* acting during LR emergence. *M. truncatula* HB1 regulates an adaptive developmental response to minimize the root surface exposed to adverse environmental stresses.

INTRODUCTION

Developmental plasticity allows higher plants having the same genotype to give rise to different phenotypes depending on environmental conditions. In contrast with animals, plants exhibit a remarkable flexibility in their architecture and growth patterns in response to external conditions, due to the continuously active shoot and root meristems and their capability to generate new organs after embryogenesis (Wolters and Jurgens, 2009). External cues influence plant growth by modulating hormone levels and signaling. The root architecture of the plant constitutes an important model to study how developmental plasticity is translated into growth responses under stress conditions. Indeed, primary root development and the formation of de novo meristems to generate lateral roots (LRs) are conditioned by the soil environment (Osmont et al., 2007). Legumes, the third major crop worldwide, can also generate on their roots other de novo meristems, so-called root nodules, through symbiotic interactions with soil bacteria (Crespi and Frugier, 2008). These organs

allow legumes to fix atmospheric nitrogen and to grow in nitrogen-poor soils. Hence, legumes are considered interesting pioneer crops for the incorporation of salty soils into agriculture as their presence may allow growth of other plant species. However, their root growth and architecture, including nodule formation, are still highly sensitive to environmental constraints, such as water availability and salt stress, resulting in a restricted productivity (Gonzalez-Rizzo et al., 2006).

Plant hormones have been shown to play primary roles in the generation of new meristems in legume roots (Gonzalez-Rizzo et al., 2006). Auxin is the key hormone for LR formation, regulating initial priming of pericycle cells via asymmetric divisions, primordium boundary formation, and root emergence (De Smet et al., 2006). The local accumulation of auxin in individual xylem pericycle cells serves as an instructive signal to select cells to initiate LRs (Dubrovsky et al., 2008). Once initiation takes place, further divisions lead to the formation of the LR primordia and the emergence of the LR from the primary root through breakage of the epidermal cells (Peret et al., 2009a, 2009b). It has also been shown that certain external cues, such as Pi starvation, regulate auxin pathways to control LR formation and emergence (Perez-Torres et al., 2008).

Besides auxin, many other positive and negative regulators participate in the determination of root architecture (Fukaki and Tasaka, 2009). The response to environmental stresses is mainly mediated by the hormone abscisic acid (ABA). In *Arabidopsis thaliana*, ABA regulates LR initiation and emergence through

¹ These authors contributed equally to this work.

² Address correspondence to crespi@isv.cnrs-gif.fr.

The author responsible for distribution of materials integral to the findings presented in this article in accordance with the policy described in the Instructions for Authors (www.plantcell.org) is: Martin Crespi (crespi@isv.cnrs-gif.fr).

^WOnline version contains Web-only data.

www.plantcell.org/cgi/doi/10.1105/tpc.110.074823

ABI3 (Brady et al., 2003; De Smet et al., 2003) and independently represses auxin response in LR primordia. The control exerted by ABA on root branching can be relevant under stress conditions to optimize root growth (De Smet et al., 2006). Indeed, ABA and drought stress have similar and probably synergistic effects on LR formation (Xiong et al., 2006).

In legumes, opposite effects of ABA at low and high concentrations (inducing and repressing, respectively) on LR formation and nodulation has been reported, and ABA-responsive mutants affecting both organs have been identified in *Medicago truncatula* (Bright et al., 2005; Liang et al., 2007; Ding et al., 2008). However, almost nothing is known about the mechanisms regulating the effect of the environment on legume root architecture. In this work, we identified a role for *HB1*, an HD-Zip I transcription factor that is responsive to salt stress in root apices (Gruber et al., 2009), in the regulation of root architecture in *M. truncatula*. In vitro DNA binding assays and bioinformatic analysis of salt-regulated promoters allowed us to demonstrate that *HB1* represses a LOB (for Lateral Organ Boundaries) domain transcription factor (TF) involved in an auxin pathway. This regulatory network is crucial for the control of LR emergence and root growth under environmental constraints in the model legume *M. truncatula*.

RESULTS

Environmental Stresses Induce the HD-Zip I TF *HB1* in *M. truncatula* Roots

To search for environmentally regulated pathways affecting meristem function, a transcriptomic approach was performed to identify TFs responding to a short-term salt stress (100 mM NaCl, 1 h) in *M. truncatula* root meristems. The TF first called HD1374 (Gruber et al., 2009; henceforth named *HB1* for *M. truncatula* homeobox 1) is one of the TFs most strongly induced by salt stress in root apices. *HB1* belongs to the HD-Zip family, characterized by the plant-specific combination of a homeodomain (HD) and a dimerization motif, the leucine zipper (Zip). *HB1* can be classified in the HD-Zip I subfamily, whose members are involved in responses to abiotic stress and ABA, blue light signaling, and deetiolation (Ariel et al., 2007). The single copy of the *HB1* gene found in the known portion of the *M. truncatula* genome and the duplicated homologous genes in *Arabidopsis* (*HB7* and *12*) share a common structure (Henriksson et al., 2005; Figure 1A). The encoded proteins are highly conserved (Figure 1B), and it was shown that *Arabidopsis* *HB7* and *12*, as well as related genes from other plant species, are expressed in roots and induced by water deficit, salt stress, and ABA (Soderman et al., 1996; Dezar et al., 2005; Ariel et al., 2007; Manavella et al., 2008). *HB1* expression responds to salt and osmotic stresses as well as ABA treatments in *M. truncatula* roots (Figure 1C). Indeed, the *HB1* promoter contains two ABA response elements and two drought response elements (Figure 1B), also present in the promoter regions of *HB1* homologs from *Arabidopsis* (*HB7* and *12*) and sunflower (*HB4*) (Soderman et al., 1996; Manavella et al., 2008). Therefore, *HB1* is regulated by environmental stresses in *M. truncatula* roots.

HB1 Regulates Root Architecture and LR Emergence in *M. truncatula*

As scarce information is available on the role of HD-Zip I TFs in roots in response to environmental stresses, we constitutively expressed *HB1* in transgenic roots of composite *M. truncatula* plants (obtained through *Agrobacterium rhizogenes* infection, composite plants harbor transgenic roots on wild-type aerial parts; Boisson-Dernier et al., 2001). In *M. truncatula* wild-type plants, low salt concentrations slightly but significantly induced root biomass growth without altering root architecture, whereas a severe repressive effect is caused at high NaCl concentrations (see Supplemental Figure 1 online). Root dry weight is significantly affected already at 50 mM NaCl (see Supplemental Figure 1C online), and this concentration was used to analyze the impact of salt stress on root growth. The overexpression of *HB1* in composite plants (Boisson-Dernier et al., 2001) resulted in a modified root system with a longer primary root and a significantly lower root dry weight (Figures 2A and 2B). The difference in root architecture became even greater when the root mass per primary root length was considered (Figure 2C). Interestingly, in contrast with control transgenics, the whole root mass of the *HB1*-overexpressing composite plants was not negatively affected by salt stress (Figure 2B; see Supplemental Figure 3A online).

The effect of *HB1* overexpression on root dry weight resembled that observed in response to the exposure of wild-type plants to high NaCl concentrations (cf. Figure 2C with 50 mM NaCl or more in Supplemental Figure 1C online). At 50 mM NaCl, the negative effect on wild-type root architecture seems mainly regulated at the LR emergence level (see Supplemental Figures 1D and 1E online) as the number of initiated LRs per centimeter is not significantly different from the controls. To define a parameter independent of any effect on LR initiation, LR emergence was monitored as the percentage of emerged LRs out of the total initiated roots (see Supplemental Figure 1E online).

A role of *HB1* in LR formation and root architecture was analyzed using two independent TILLING-derived *HB1* mutant lines (Le Signor et al., 2009). The *hb1-1* allele carries a stop codon in the third helix of the HD, involved in DNA recognition, and a second allele, *hb1-2*, present in a heterozygous line exhibits a point mutation in the third helix of the HD (Figures 1A and 1B). The latter mutation should prevent the TF from efficiently binding to DNA. The root architecture phenotypes of these mutants were first analyzed under control conditions (Figures 2D to 2F). The total number of initiated LRs was determined by microscopy inspection of the whole root system. The LRs were considered as emerged only when they had broken the epidermal cell layer, whereas all the LR primordia present in roots were counted, from the four-cell stage on (according to *Arabidopsis* stages II to VII; Malamy and Benfey, 1997). This analysis revealed that the number of initiated primordia per centimeter is not significantly affected in *hb1-1* plants (Figure 2E). By contrast, a significant increase (i.e., almost 30%) in LR emergence was detected in these mutants (emerged roots/cm; Figure 2F). As the LR histology was similar to the wild type, this phenotype in LR emergence was likely not due to any major developmental defect in LR meristems or differentiation. Cosegregation analysis of the

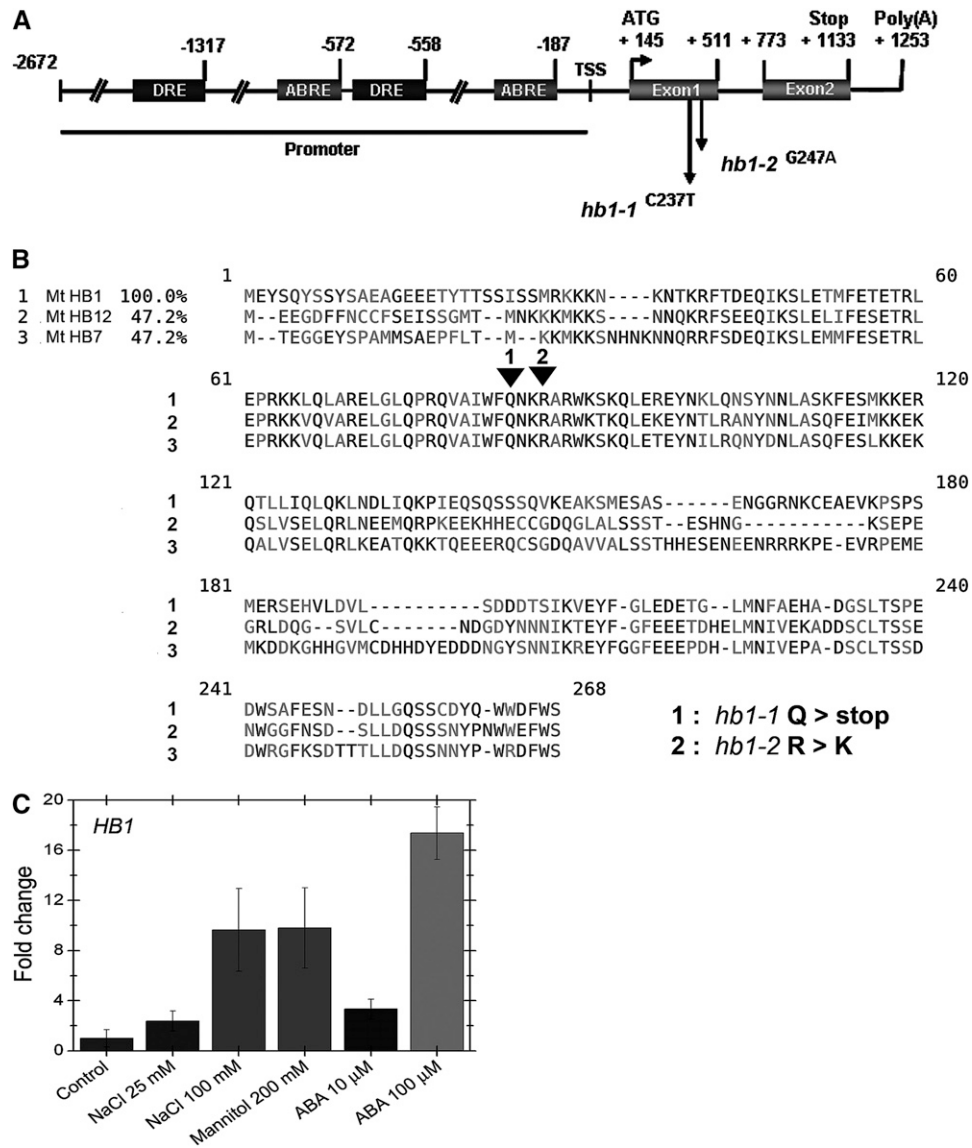


Figure 1. HB1 Encodes an HD-Zip I TF Regulated by ABA, NaCl, and Mannitol.

(A) HB1 gene structure and promoter region highlighting the location of the ABA response elements (ABREs) and drought response elements (DREs). TSS, transcription start site. Arrows indicate position of *hb1-1* and *-2* alleles obtained through TILLING and the nucleotide substitutions. Numbers indicate distances from the transcription start site.

(B) Protein alignment of HB1 with *Arabidopsis* HB7 and 12. Identity is indicated on the left side as a percentage relative to the HB1 sequence used as reference. The alignment was performed with MAFFT 6.0 (Katoh and Toh, 2008) and the visualizing tool MView (Brown et al., 1998). The *hb1-1* and *-2* mutations obtained by TILLING are indicated using arrowheads, and the protein sequence modifications are shown below the alignment.

(C) Real-time RT-PCR analysis of HB1 expression in response to different concentrations of NaCl, ABA, and mannitol. Bars express the fold change on a linear scale. *H3L* was used as reference gene, and ratios were normalized against the control (nontreated) condition. Error bars represent SD of four biological replicates.

heterozygous *hb1-2* allele also showed a significant increase in LR emergence in homozygous mutants (Figure 2H). As legumes are able to interact with symbiotic bacteria, we analyzed the behavior of the *hb1* mutants under symbiotic conditions. At 7 d after inoculation with *Sinorhizobium meliloti*, *hb1-1* mutants displayed significantly shorter main roots and a higher increase

in the emerged LR density (40%; Figure 2G) than plants grown in the presence of fixed nitrogen. Nodule development and morphology were similar to the wild type, and their number per centimeter of root was not significantly reduced in the mutant (see Supplemental Figure 2 online). Altogether, these results show that *HB1* affects *M. truncatula* root architecture.

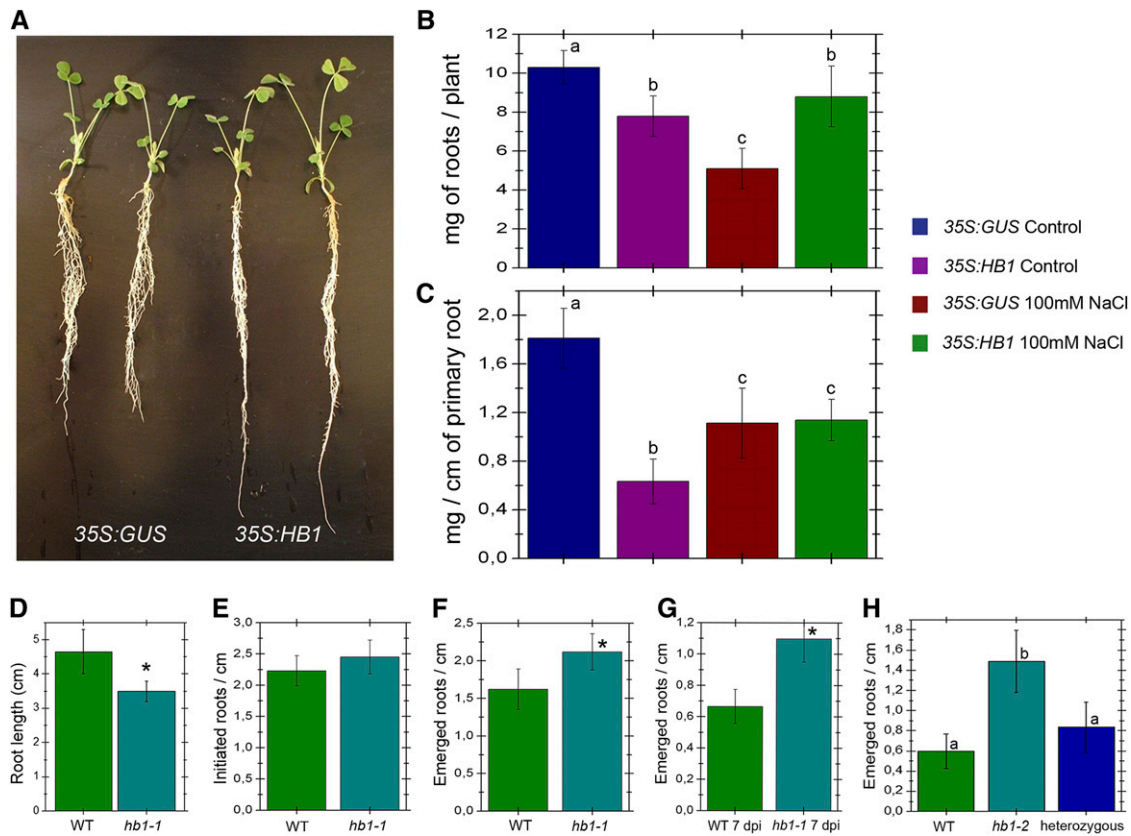


Figure 2. Plants Affected in HB1 Function Exhibit Perturbed Root Architecture.

(A) Two representative composite *M. truncatula* plants transformed with 35S:GUS and 35S:HB1 constructs after 4 weeks of growth in sand/perlite (greenhouse).

(B) and (C) Root dry weight per plant (B) and per centimeter (C) of primary root was quantified under control and salt stress (100 mM NaCl) conditions. The letters indicate mean values significantly different between groups (Kruskal-Wallis test $P < 0.05$, $n > 20$ in every case).

(D) Primary root length was measured for wild-type and *hb1-1* mutant plants.

(E) to (G) Quantification of LR initiation and emerged LRs per centimeter of primary root in *hb1-1* mutants and the wild type.

(E) Total number of initiated LR per centimeter in plants growing in nitrogen-containing medium.

(F) and (G) Percentages of emerged LR per centimeter of primary roots in the wild type and *hb1-1* mutants in the same medium (F) and 7 d after inoculation with *S. meliloti* in a nitrogen-poor medium (symbiotic conditions) (G).

In (B) to (F), $n > 20$ per construction and condition per experiment. The asterisks indicate mean values significantly different between the wild type and *hb1* mutants (for [D] to [G], Student's *t* test, $P < 0.01$, error bars represent SD between biological replicates).

(H) Segregation analysis of the *hb1-2* mutation. The number of emerged LRs per centimeter was determined in heterozygous, homozygous mutant, and wild-type sibling plants from a 3-week-old segregating *hb1-2* population ($n = 12$ homozygous, 20 heterozygous, and 10 wild-type siblings; Kruskal-Wallis test, $P < 0.05$). Letters indicate mean values significantly different between groups.

HB1 Regulates LR Emergence under Environmental Stress Conditions in *M. truncatula*

To further characterize the action of HB1 in LR emergence, we analyzed the physiological response of wild-type and *hb1-1* plants to NaCl and ABA concentrations affecting root architecture. In control conditions, the *hb1* plants exhibited a larger number of emerged roots than the wild type as previously mentioned (Figure 2; see Supplemental Figure 3A online). Microscopy analysis of these roots after lugol staining showed that both primary and LRs have similar morphologies (see Supplemental Figure 3B online). ABA and salt treat-

ments modified root architecture in *M. truncatula* to varying extents (see Supplemental Figure 1 online; Liang et al., 2007). The density of initiated LRs and the percentage of emerged LRs were determined in plants grown for 6 d in different concentrations of salt and ABA (Figure 3). The results showed that 10 μ M ABA induced LR initiation in wild-type and *hb1* plants (Figure 3A). The other treatments negatively affect LR emergence (such as 50 μ M ABA and 50 or 75 mM NaCl) but similarly affected LR initiation in wild-type and *hb1-1* plants. By contrast, regarding LR emergence, *hb1* mutants were insensitive to the positive effect exerted by 10 μ M ABA or the negative effect of higher ABA or salt concentrations (Figure 3B). In

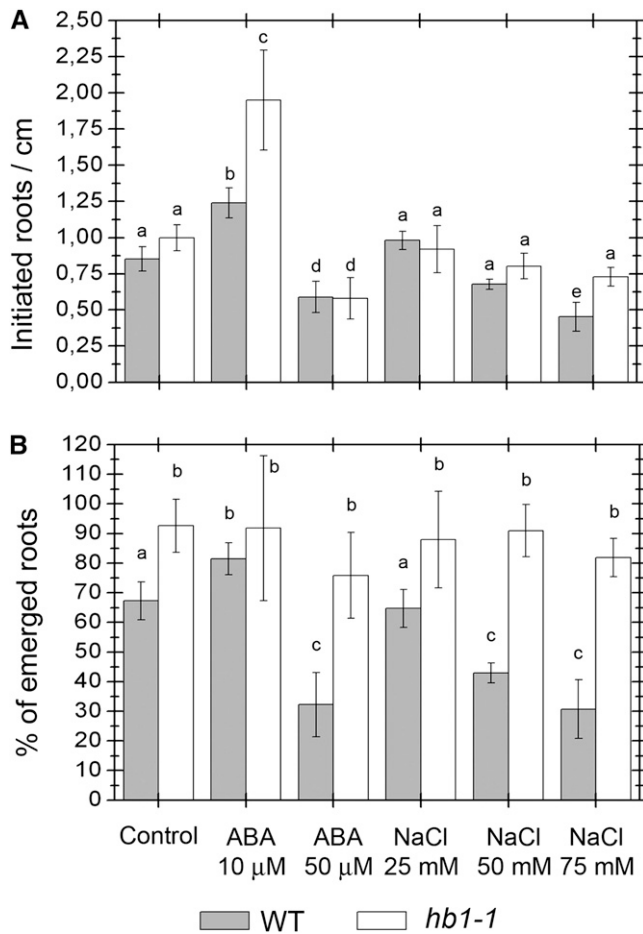


Figure 3. *HB1* Regulates LR Emergence in *M. truncatula*.

Total initiated LR per centimeter of primary root (**A**) and percentage of emerged roots (relative to the total number of initiated roots; **B**) for the wild type and *hb1-1* mutants in presence of different concentrations of ABA and NaCl. In all treatments, the percentage of emergence in *hb1-1* mutants was similar ($n > 20$ per experiment; Kruskal-Wallis test, $P < 0.05$). The letters indicate mean values significantly different between groups. Error bars represent SD between three biological replicates.

contrast with the wild type, the emergence ratio then remained unaffected in the *hb1* mutant plants in all treatments. Interestingly, microscopy analysis of these roots revealed a defect in primary meristem organization in *hb1-1* plants when exposed to salt stress (see Supplemental Figure 3B online). A similar defect in meristem organization is observed in wild-type LRs once emerged in a salty environment. Histological analysis of *hb1-1* root apices under salt stress conditions showed the absence of a root cap and the lack of amyloplasts in these primary roots, in contrast with the normal histology of *hb1-1* roots observed under control conditions (see Supplemental Figure 4 online). Altogether, these results clearly indicated that the effect of ABA and salt on LR emergence and root architecture involves the action of *HB1*.

HB1* Represses the Expression of the Auxin-Regulated LOB-Like TF *LBD1

To unravel how *HB1* regulates LR emergence in response to environmental stress, we searched for *HB1*-targeted genes. To this end, we expressed the *HB1* HD-Zip domain in bacteria as a glutathione *S*-transferase fusion. After purification by affinity chromatography, we performed competition electrophoretic mobility shift assays. The recombinant protein recognized the pseudopalindromic sequence CAATNATTG with the highest affinity in vitro (see Supplemental Figures 5A and 5B online), as reported for members of the HD-Zip I subfamily in other plant species (Soderman et al., 1996; Palena et al., 1998). To identify candidate target genes, we scanned for the sequence CAATNATTG in the promoter regions of genes coregulated with *HB1* in the previous transcriptomic analysis of salt stress responses in root apices (Gruber et al., 2009). A group of 12 candidate target genes arose (see Supplemental Table 1 online). We focused our study on three genes that were strongly induced and one that was strongly repressed by salt stress in root apices (fold change > 10). Only the salt-repressed gene was also downregulated in the *HB1*-overexpressing roots under the control conditions (Figure 4A), whereas the three other tested genes were not affected in these roots (see Supplemental Figure 6 online). Furthermore, transcript levels of this *HB1*-repressed target gene were significantly higher in the *hb1-1* mutant when compared with the wild type (Figure 4A, right panel). This gene codes for a LOB-like TF (Shuai et al., 2002; Husbands et al., 2007; henceforth called *LBD1* for LOB-Binding Domain 1) and has a CAATAATTG *cis*-element 1507 bp upstream of its ATG (and 944 bp upstream the TSS; Figure 5A). Complementation of *hb1-1* mutant roots with a 35S:*HB1* construct restored *LBD1* expression levels (Figure 4B). Several TFs from the LBD family have been recently described as being involved in adventitious and LR formation in cereals (Liu et al., 2005), whereas in *Arabidopsis*, *LBD16* and 29 are targets of ARF7 and 19, two auxin response factors (Okushima et al., 2005). Considering that *LBD* genes positively regulate LR formation, the molecular phenotype of *LBD1* in *hb1* and 35S:*HB1* plants may be linked to the effect of *HB1* on root system morphology.

Direct Repression of *LBD1* Expression by *HB1* Is Associated with LR Formation

The spatial expression patterns of *HB1* and *LBD1* were determined using promoter fusions to the β -glucuronidase (*GUS*) reporter gene in *M. truncatula* roots. In basal conditions, the *HB1* promoter drove strong *GUS* activity during different stages of LR formation (Figure 4C). The *LBD1* promoter was also active during LR formation but at much lower levels (Figure 4D). Histological sections of stained roots showed overlapping expression of *HB1* and *LBD1* in the LR primordial, whereas in the emerged LR, they may be in contiguous cells as *LBD1* remains at the LR base (Figure 4E). Hence, *HB1* may repress *LBD1* at several stages of LR formation in *M. truncatula*. Besides, in contrast with *LBD1*, *ProHB1:GUS* fusions were also expressed in the root apex, young nodules, and vascular tissues of the mature nodule (see Supplemental Figure 7 online). Treatments with ABA and NaCl strongly enhanced *ProHB1* activity in LRs (see Supplemental

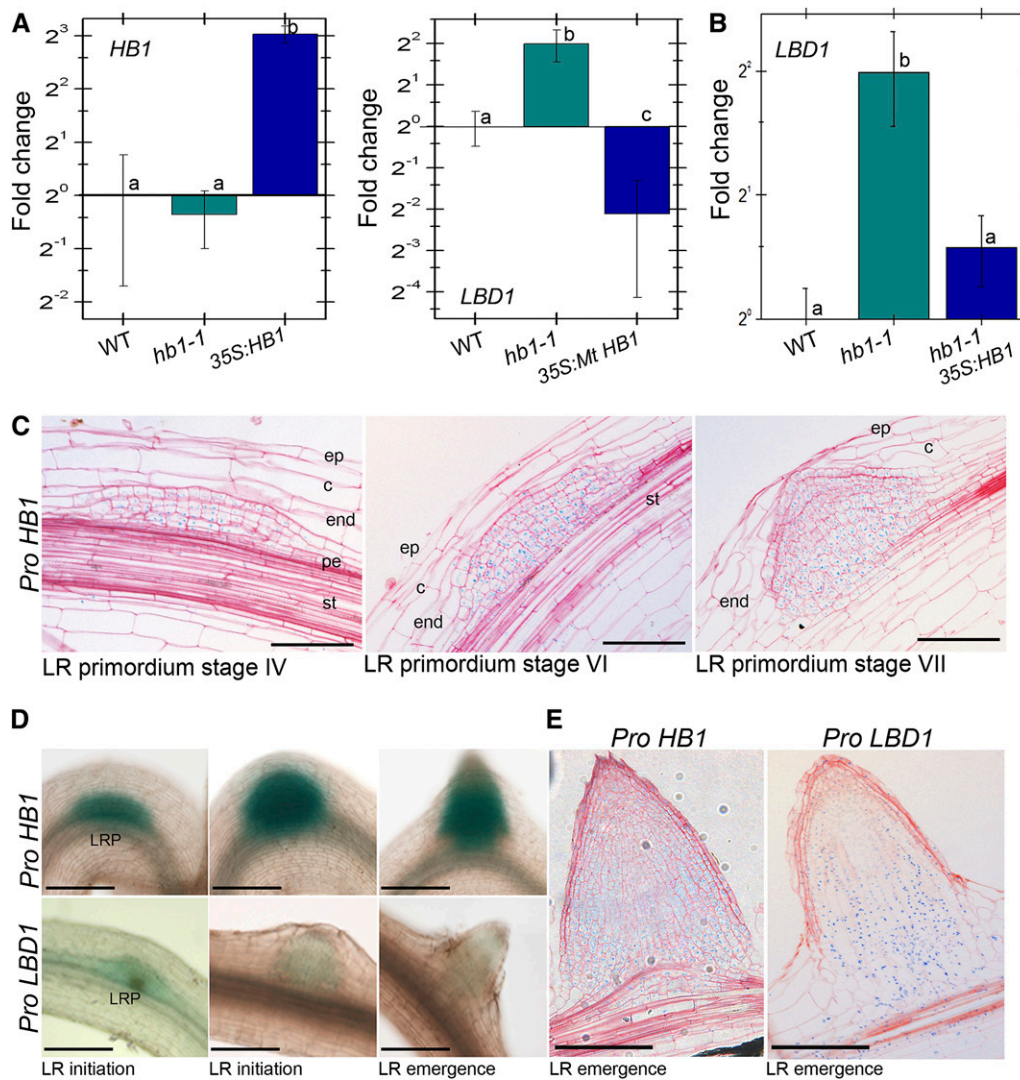


Figure 4. The LOB-Like *LBD1* TF Gene Is Transcriptionally Repressed by HB1.

(A) Real-time RT-PCR analysis of *HB1* (right panel) and *LBD1* (left panel) transcript levels in *hb1-1*, *35S:HB1*, and wild-type roots.

(B) Real-time RT-PCR analysis of *LBD1* expression in wild-type and *hb1-1* roots transformed or not with a *35S:HB1* construct. Bars in **(A)** and **(B)** express the fold change on a log₂ scale. The *H3L* gene was used as reference gene, and ratios were normalized against the reference genotype (wild type). Error bars represent SD for three biological replicates.

(C) *HB1* expression pattern in different stages of lateral root primordia analyzed by detecting GUS activity in roots transformed with a *ProHB1*:GUS construct. ep, epidermis; c, cortex; end, endodermis; pe, pericycle; st, stele.

(D) Comparative expression patterns of *HB1* (top row) and *LBD1* (bottom row) promoters during LR formation. The low level of expression of *LBD1* in transgenic root carrying *ProLBD1*:GUS fusions is noteworthy. LRP, LR primordia. Bars = 250 μ m.

(E) Histological sections of *ProHB1*:GUS and *ProLBD1*:GUS emerged LR primordia are shown. Bars = 125 μ m.

Figures 7E and 7F online). Strikingly, when the *ProLBD1*:GUS construct was introduced in *hb1-1* mutant roots, GUS staining was detected in every root region normally expressing *HB1*, such as the LR primordia and the root apex (Figure 5B). No *ProLBD1*:GUS activity was detected in nodules of these plants. The functionality of the *cis*-acting element recognized in vitro by HB1 on the *LBD1* promoter was tested through site-directed mutagenesis in wild-type roots (Figure 5B, bottom row). This mutagenesis

prevents HB1 binding (see Supplemental Figure 5C online). The resulting expression pattern resembled that observed in *HB1* plants, demonstrating that repression of *LBD1* expression requires this *cis*-motif. In addition, chromatin immunoprecipitation assays followed by PCR (ChIP-PCR) were performed in roots harboring the *ProHB1*:*HB1*:2xHA construct. To detect the direct binding of the HB1-HA fusion protein to the *LBD1* promoter, these roots were treated for 1 h with 100 mM NaCl. ChIP-PCR

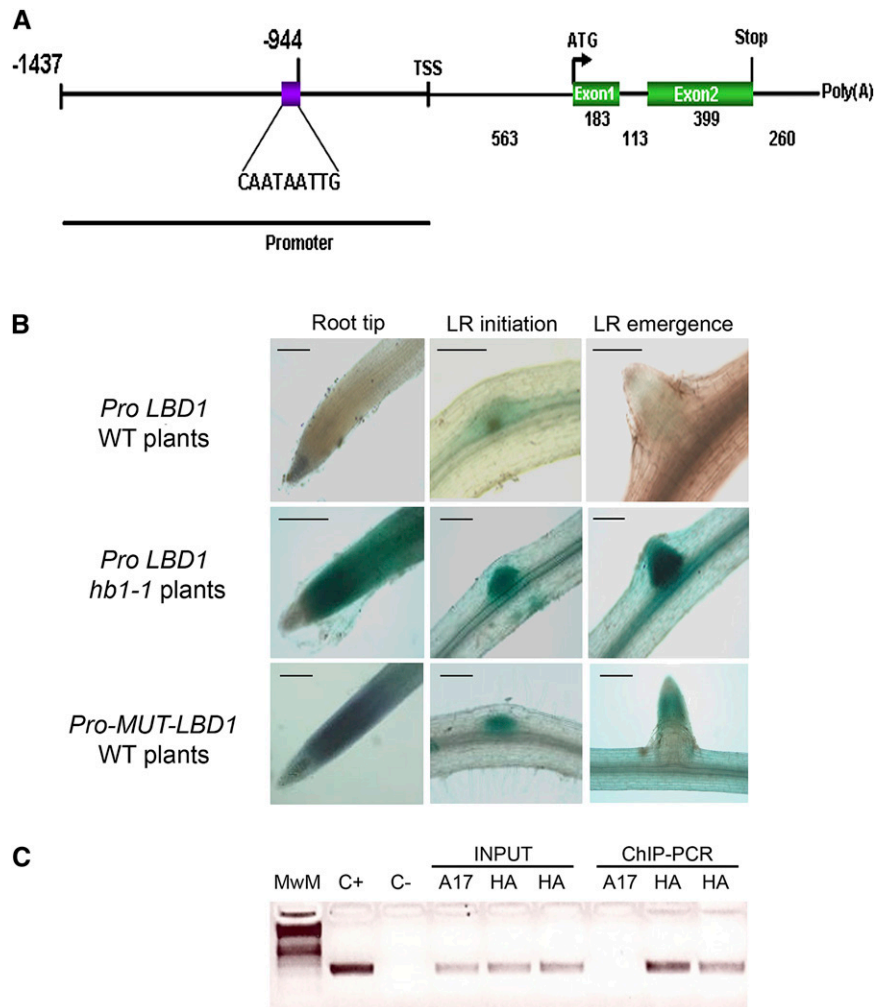


Figure 5. The *LBD1* Promoter Contains a Specific *cis*-Acting Element Required for *HB1* Regulation.

(A) Scheme of the *LBD1* promoter region and gene structure highlighting the location of the *cis*-acting element CAATAATTG. TSS, transcription start site.

(B) Analysis of *ProLBD1*:GUS activity in wild-type and *hb1-1* roots (top and middle rows) and the effect of site-directed mutagenesis of the *cis*-element on the *LBD1* promoter activity (*Pro-MUT-LBD1*) in wild-type roots (CAATAATTG was replaced by CAGGATCCG; bottom row). Bars = 250 μ m.

(C) ChIP-PCR analysis using *LBD1* primers spanning the promoter region containing the specific *cis*-acting element required for HB1 regulation. The indicated results were obtained from samples precipitated with α -HA antibody. Lane 1, molecular weight marker; lane C+, *LBD1* BAC clone positive control; lane C-, water negative control. ChIP-PCR assays were done on 3-week composite plants untransformed (A17) or transformed with a *ProHB1*:*HB1*:2XFLAG:2XHA construct (HA). INPUT, total nuclei sample before immunoprecipitation; ChIP-PCR, after immunoprecipitation with HA antibodies. Two independent clones expressing the *HB1*-HA fusion but not the A17 control give a positive signal for the *LBD1* promoter.

assays using α -HA antibodies confirmed that HB1 directly binds to *ProLBD1* (Figure 5C). Altogether, these results suggest that HB1 may control *M. truncatula* LR emergence in response to the environment by directly repressing *LBD1* transcription.

Opposite *HB1* and *LBD1* Expression Patterns Correlate with the Effect of Environmental Stresses on Auxin Action during LR Emergence

To analyze how HB1-dependent environmental control of the *LBD1* auxin-related pathway may take place in *M. truncatula*

LRs, the long-term physiological effects of salt, ABA, and auxin were analyzed. Physiological effects were analyzed both at the level of LR initiation and emergence. Germinated wild-type plants (3 d) were transferred to plates with medium supplemented with the corresponding hormone and/or salt for 6 d (Figure 6). Indole-3-acetic acid (IAA) mainly induced LR initiation without considerably affecting LR emergence (green bars in Figures 6B and 6C). As previously shown (Liang et al., 2007), 10 μ M ABA slightly but significantly induced both LR initiation and emergence in legumes (Figures 6B and 6C, brown bars; Liang et al., 2007). On the other hand, 50 μ M ABA had a drastic

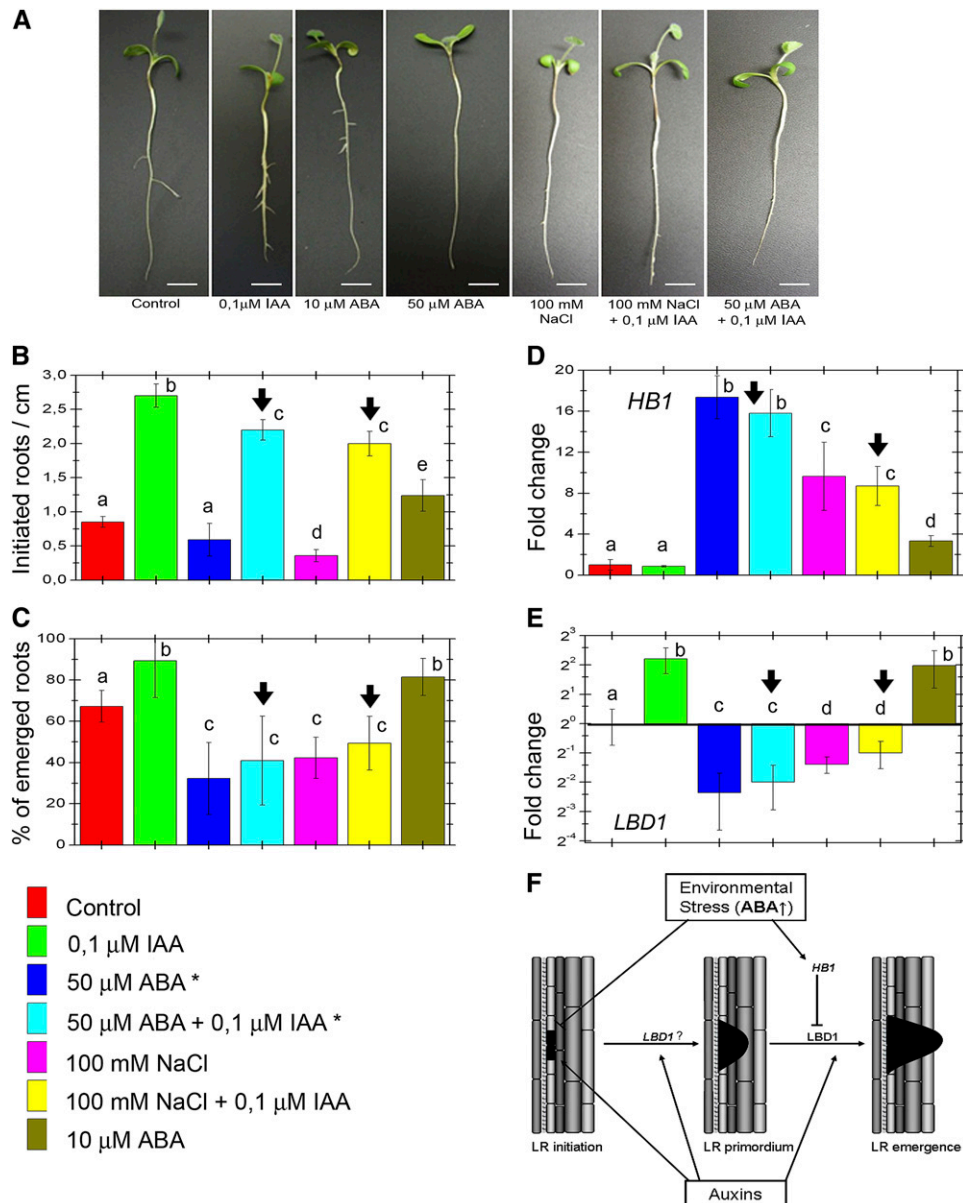


Figure 6. Morphological and Molecular Responses of Wild-Type Plants to Auxin, ABA, and Salt Treatments.

(A) Representative plants showing the long-term physiological effects of auxin (IAA), ABA, and salt on *M. truncatula* root architecture. Plants (3 d old) were grown for 6 d in plates supplemented with ABA, IAA, NaCl individually, or in combination. Bars = 1 cm.

(B) and **(C)** Total LR initiation per centimeter of primary root **(B)** and percentage of LR emergence **(C)** in wild-type *M. truncatula* plants after 6 d of the different treatments specified by each color. The asterisks indicate that for the short-term molecular studies, 100 μ M ABA was applied ($n > 20$ per condition; Kruskal-Wallis test, $P < 0.05$). The letters indicate mean values significantly different between groups. Error bars are SD between biological replicates.

(D) and **(E)** Real-time RT-PCR analysis of expression levels (similar barcode as **[B]** and **[C]**) for *HB1* **(D)** and *LBD1* **(E)** in wild-type plants in response to short-term IAA, ABA, or salt treatments (3 h). Bars express the fold change on a linear and a log₂ scale, respectively. Error bars are SD in three biological replicates. Arrows indicate the most relevant results referred to in the text.

(F) Proposed role for *HB1* in LR emergence. Three stages for LR formation (initiation, primordial formation, and emergence) are schematized. *HB1* represses *LBD1* expression in the LR primordia. When *M. truncatula* is exposed to salt stress or high ABA concentrations, *HB1* controls LR emergence, likely by repressing *LBD1*. *HB1* mediates a developmental plasticity response to adapt root architecture to environmental constraints.

repressive action both on root initiation and emergence comparable to the effect of 100 mM NaCl (Figures 6B and 6C, dark-blue and pink bars). The repression of LR emergence caused by high concentrations of ABA or NaCl could not be reverted even when initiation was strongly activated by auxin (Figures 6B and 6C, light-blue and yellow bars).

We then analyzed the molecular behavior of *HB1* and *LBD1* in response to short-term treatments (3 h) with the same hormones and salt combinations (Figures 6D and 6E). Treatment with IAA provoked a significant induction of *LBD1* transcription, in accordance with previous reports in *Arabidopsis* (Okushima et al., 2005; Figure 6D, green bars). Low concentrations of ABA (10 μ M), which have a positive effect on LR formation (Figure 6A), strongly upregulated *LBD1*, whereas *HB1* was slightly induced (Figures 6D and 6E, brown bars). By contrast, after short treatments with high ABA and NaCl concentrations, *HB1* and *LBD1* were oppositely regulated, being strongly induced and repressed, respectively (Figures 6D and 6E, dark-blue and pink bars). Remarkably, the *LBD1* expression in response to IAA applied together with higher ABA or NaCl concentrations resembled those without IAA (Figures 6D and 6E, light-blue and yellow bars; indicated by arrows). Furthermore, GUS fluorometric measurements of roots transformed with *ProLBD1:GUS* and *Pro-MUT-LBD1* revealed that the repression exerted by ABA is dependent on the CAATAATTG cis-motif recognized by *HB1* (see Supplemental Figure 8 online).

Overall, the *HB1* and *LBD1* expression profiles by auxin and ABA were consistent with the long-term phenotypes provoked by both hormones on LR initiation and emergence as well as with the *hb1* mutant phenotype. Even in the presence of IAA, high ABA or NaCl (strongly inducing *HB1*) significantly repressed LR emergence (but not initiation) and *LBD1* (Figure 6, red arrows). This opposite correlation between *HB1* and *LBD1* further supports that *HB1* represses the auxin-regulated TF *LBD1* to control LR emergence in *M. truncatula*.

DISCUSSION

Due to their sessile nature, plants need to adapt their postembryonic development to specific environmental conditions, a characteristic that has a major impact on crop production. Here, we identify the function of *HB1* in the regulation of LR emergence and demonstrate a direct molecular link between this environmentally responsive TF and the repression of the auxin-induced LOB domain TF, *LBD1*, in *M. truncatula*. This regulatory module notably acts in root meristems and may represent a crosstalk between auxin and ABA signaling pathways.

The increasing interest in crop and model legume genomes (Choi et al., 2004; Cannon et al., 2009) reflects their agronomic importance worldwide. Even though several TFs in legumes are linked to abiotic stresses, nutrient availability, and nitrogen-fixing symbiosis, their molecular mechanisms of action remain largely unknown (Udvardi et al., 2007). Interestingly, although several HD-Zip I TFs have been linked to abiotic stresses (Ariel et al., 2007), only one HD-Zip I TF identified through genetic analysis was shown to regulate the formation of tendrils, a specific leaf-related structure in pea (*Pisum sativum*; Hofer et al., 2009). No

root phenotype was reported for this mutant. We have identified *hb1* mutants that are globally affected in root architecture in *M. truncatula*. The anatomy of both root lateral organs, LRs and nodules, is normal in *hb1* mutants, but the number of emerged LRs is increased. The phenotype of increased LR numbers was described in the cytokinin-insensitive *cre1* and ethylene-insensitive *skl* mutants (Gonzalez-Rizzo et al., 2006; Penmetsa et al., 2008). However, these mutants are also affected in nodule density (nodule number per root centimeter). The *har1 Lotus japonicus* supernodulator mutant also exhibits increased LR formation (Wopereis et al., 2000), whereas the *M. truncatula latd* mutant fails to differentiate both LRs and nodules (Bright et al., 2005; Liang and Harris, 2005; Liang et al., 2007). *LATD* has been recently identified as a member of the *NRT1* transporter family, and its expression is repressed by auxin and ABA (Yendrek et al., 2010). The *hb1* mutant reveals a different regulatory pathway of legume root architecture with normal nodulation and increased LR emergence. The primary root of the *latd* plants exhibits a defect in root apex organization, with a reduced accumulation of amyloplasts in the root cap under control conditions (Liang et al., 2007). This phenotype is rescued by applying 10 μ M ABA. By contrast, we detect a disorganization of the primary root apex, showing reduced amyloplast accumulation, only under salt stress, a condition inducing ABA production. This defect may further explain the enhanced LR emergence phenotype observed under salt stress. Nevertheless, even in control conditions, *HB1* plays a significant role in LR emergence.

The *hb1* LR phenotype can be due to derepressed expression of *LBD1* in these plants. In *Arabidopsis*, *LBD* genes have been described as being involved in LR initiation and patterning, just before the emergence event, whereas *LBD16* and *LBD18* are regulated by auxin through ARF7 and ARF19 (Okushima et al., 2005; Lee et al., 2009; Peret et al., 2009b). Although there are no *Arabidopsis*-like auxin-responsive cis-elements in the *M. truncatula LBD1* promoter region, its expression is regulated by auxins. The *LBD* genes may take part in alternative pathways in other plant species as their closest homologs in rice (*Oryza sativa*) and maize (*Zea mays*) participate in shoot-borne root formation (Hochholdinger and Zimmermann, 2008). Interestingly, the phylogenetic tree of At LBDs and the predicted Mt LBDs (see Supplemental Figure 9 and Supplemental Data Set 1 online) shows that *M. truncatula LBD1* is in between the two classes previously defined (Shuai et al., 2002), preventing a prediction of a functional *Arabidopsis* ortholog. However, one of the closest *Arabidopsis* Class II genes involved in nitrogen metabolism (Rubin et al., 2009), *LBD37*, contains a CAATAATTG cis-element in the proximal promoter region. As *Arabidopsis HB1* and *12* are strongly induced by ABA in roots (Soderman et al., 1994; Olsson et al., 2004; Ariel et al., 2007), the repression of auxin-responsive genes in response to environmental cues may be driven by a conserved regulatory pathway. ChIP-PCR assays reliably monitor direct interactions of TFs with their targets and have unraveled regulatory networks acting in nodule organogenesis in the legume (Hirsch et al., 2009).

The role of auxin in LR initiation, patterning, and emergence is well known (Fukaki and Tasaka, 2009; Peret et al., 2009a, 2009b). The crucial role of auxin in LR emergence was recently highlighted by the characterization of the auxin influx carrier LAX3 in

Arabidopsis (Swarup et al., 2008). Modulation of auxin transport and signaling in cells adjacent to the LR primordium induces specific activation of enzymes leading to the cell wall loosening required for LR emergence. It has also been recently described how Pi starvation may control LR formation and emergence by changing auxin responsiveness depending on the TRANSPORT INHIBITOR RESISTANT1 auxin receptor (Perez-Torres et al., 2008). In addition, in *Arabidopsis*, ABA and auxin signaling pathways share certain actors, including TFs such as ABI3 (Brady et al., 2003). ABI3 is auxin inducible in LR primordia, and *abi3* mutants show reduced LR initiation in response to auxin. The direct molecular link between *HB1* and *LBD1* combines an ABA-responsive TF that represses an auxin-inducible TF, as ABI3. In fact, ABA plays a central role in mediating the regulatory effects of nitrate on root branching and architecture in *Arabidopsis* (Signora et al., 2001). Our results show how an abiotic stress recruits an ABA-dependent HD-Zip I TF to repress an LBD-dependent pathway and determine root architecture in *M. truncatula*. We propose that *HB1* could be an element of the complex interaction of ABA and auxin signaling in roots (Osmont et al., 2007). The induction of *HB1* by external cues represses the emergence of new LRs and diminishes the exposed surface of the root system to the stressing constraint (Figure 6F). Hence, *HB1* controls root developmental plasticity, and the identification of *LBD1* function and target genes may further build the regulatory network by which auxin and ABA regulate LR emergence in *M. truncatula* and more generally in legumes.

METHODS

Plant Material, *Agrobacterium rhizogenes* Transformation, and Treatments

Medicago truncatula Jemalong A17 seeds were sterilized, grown, and transformed as previously described (de Lorenzo et al., 2009). Two *M. truncatula* TILLING *HB1* mutants were obtained (Le Signor et al., 2009) and genetically characterized.

Germinated *M. truncatula* A17 seeds were transferred to square plates with Fahræus medium (Truchet et al., 1985, with 1.5% Bacto-Agar (Gibco) containing increasing concentrations of NaCl, ABA, IAA, or their combinations. Phenotypes were scored 6 d later. To evaluate the effect of NaCl on root growth, germinated seeds were transferred to perlite:sand (3:1, v/v) pots and irrigated with Fahræus medium containing 0, 25, 50, 75, or 100 mM NaCl. The root system and the aerial part at 21 d were dried and weighed individually. To score the phenotypes in all treatments, three biological replicate experiments were performed, including at least 20 plants per genotype and/or condition, and a Kruskal-Wallis test (Georgin and Gouet, 2000; $P < 0.05$.) was used to determine significant differences among plant populations, except in Figures 2D to 2G where a Student's *t* test was used.

Constitutive *HB1* Expression in *M. truncatula* Roots

A full-length Mt *HB1* cDNA was amplified from salt-treated *M. truncatula* roots (Gruber et al., 2009) with the primers HB1cDNAF, 5'-GGGCTCA-GAATGGAATATAGCCAATA-3', and HB1cDNAR, 5'-GGGGGATCCT-CAAGACCAAAGTCCACCATTG-3', and cloned into the binary plasmid pMF2 (containing a 35S cauliflower mosaic virus promoter; Merchan et al., 2007). Control and *HB1*-overexpressing constructs were

introduced into *M. truncatula* composite plants (Boisson-Dernier et al., 2001) and grown in pots containing perlite:sand (3:1, v/v, 10 seedlings per pot, five of each genotype) and irrigated with or without 100 mM NaCl (de Lorenzo et al., 2009). After 15 d, plants were taken out of the soil and roots imaged using ImageJ software (<http://rsbweb.nih.gov/ij/>). Aerial and root tissues were then dried and weighed. For 35S:*HB1*-transformed roots, a minimum of 10 independent transgenic roots per construction was pooled and three independent biological replicates, with three technical replicates each, were performed.

Analysis of Root Architecture Phenotypes

LR initiation and emergence were scored on germinated seedlings after 1 week in Fahræus (Truchet et al., 1985) medium. LR initiation was scored under the microscope by inspection of the whole root system (from four cells up to emerged LRs). Emerged LRs were counted as the number of LRs breaking epidermal cell layer, and its ratio against total initiation was considered as the percentage of emergence. Results were expressed as initiated or emerged LRs per centimeter of primary root (density) or percentage of emergence (independent of any effect in LR initiation). For nodulation phenotypes, germinated seeds were infected with *Sinorhizobium meliloti* 2011 (as in Gonzalez-Rizzo et al., 2006), and LRs and nodules were counted at 7, 11, and 16 d after inoculation. In all treatments, three biological replicate experiments were performed, including at least 20 plants per genotype and/or condition, and a Kruskal-Wallis test ($P < 0.05$) was used to determine significant differences among plant populations or a Student's *t* test ($P < 0.01$) when only two samples were compared.

Gene Expression Analysis

For gene expression analyses in response to salt and hormones, *M. truncatula* germinated seedlings were grown on liquid medium in a shaking incubator (125 rpm) at 24°C under long-day conditions (16 h light/8 h dark). After 7 d, seedlings were treated for 3 h with NaCl (Sigma-Aldrich), IAA (Sigma-Aldrich), ABA (Sigma-Aldrich), or combinations under the same growth conditions. Roots were then collected and immediately frozen in liquid nitrogen for RNA extraction. Total RNA and real-time RT-PCR was done as before (de Lorenzo et al., 2009) using the LightCycler real-time PCR system (Roche). A negative control without cDNA template was always included. In every case, three genes were used as reference: *ACT* (primers AFwd, 5'-TGGCATCACTCAGTAC-CTTCAACAG-3', and ARev, 5'-ACCCAAAGCATCAAATAAAGTCA-ACC-3'), *H3L* (primers H3Fwd, 5'-ATTCCAAAGCGGCTGCATA-3', and H3Rev, 5'-CTTTGCTTGGTGTCTTTAGATGG-3'), and *RBP1* (primers RBFwd, 5'-AGGGGCAAGTTCCTTCATT-3', and RBRev, 5'-AAACGG-ACGGAAAATGTGAG-3') (Gruber et al., 2009). geNorm v3.5 software (Vandesompele et al., 2002) was used to determine that *H3L* and *RBP1* could be used to determine expression ratios in figures. Three technical replicates and three independent biological replicates were performed in each experiment. Primers used for *HB1* were as follows: HB1F, 5'-GAGGCTGAGGTGAAACCAAG-3', and HB1R, 5'-ACCATCAGCATG-TTCAGCAA-3'. *LBD1* was amplified with the primers LBDF, 5'-GGTTGCCGAGTTTTGAGAAA-3', and LBDR, 5'-GGGATGAA-CAGGTGAAAGGA-3'.

GUS Histochemical and Histological Analysis

For promoter analyses, a 2817- and a 2000-bp region upstream of the ATGs of *HB1* and *LBD1*, respectively, were cloned into the gateway vector pKGWFS7 containing the GUS reporter (Karimi et al., 2002). The *HB1* promoter region was amplified using the primers 5'-CCACAAAATTTT-CCAAAAAATTC-3' and 5'-TTGAGTCTTATCATGAGGGG-3' and cloned into the pENTR/D-TOPO vector (Invitrogen). To amplify the

LBD1 promoter region, we used the oligonucleotides 5'-GGGGA-CAAGTTTGTACAAAAAGCAGGCTTAATGGAACAAATAGTAATTTG-3' and 5'-GGGGACCCTTTGTACAAGAAAGCTGGGTTTTAGTTAATCA-TGTGAACAAAG-3'. To generate *Pro-MUT LBD1*, site-directed mutagenesis was used to replace the CAATAATTG *cis*-element by CAGGATCCG using PCR nested amplifications. Then, both *LBD1* promoter versions were moved to pKGWFS7 (Karimi et al., 2002).

Transgenic roots containing *ProHB1:GUS* or *ProLBD1:GUS* and *Pro-MUTLBD1* were vacuum infiltrated, stained, and cleared as described (de Lorenzo et al., 2009) for 2 and 16 h, respectively, because *LBD1* is expressed at lower levels than *HB1*. Stained roots were observed under a microscope (Nikon AZ100 equipped with a Nikon DS-Ri1 digital camera) and/or used for histological analysis. For nodules, after embedding in 6% agarose, vibratome longitudinal sections (100 μ m; Leica VT1200S) were observed under the microscope as described before (Gonzalez-Rizzo et al., 2006). For histology, GUS-stained samples were dehydrated with a graded ethanol series, embedded in Technovit 7100 resin (Kulzer and Co.), and thin sections (7 μ m, cut on a microtome Leica RM 2155) were stained with ruthenium red (0.005%, 5 min; Sigma-Aldrich), rinsed in distilled water, air-dried, and mounted with Eukitt (Agar Scientific). Slides were observed under a microscope (Nikon AZ100/Nikon DS-Ri1 digital camera). GUS staining was representative of at least 25 independent transgenic roots in each experiment.

For lugol staining, roots were clarified for 1 min in 50% NaClO, incubated 5 min with lugol (Sigma-Aldrich), and finally washed with water (Bright et al., 2005).

GUS Activity Assays

Specific GUS activity in protein extracts was measured using the fluorogenic substrate 4-methylumbelliferyl β -D-glucuronide essentially as described by Welchen and Gonzalez (2005). Total protein extracts were prepared by grinding root tissues in extraction buffer (50 mM sodium phosphate, pH 7.0, 10 mM EDTA, 10 mM β -mercaptoethanol) containing 0.1% (w/v) SDS and 1% Triton X-100, followed by centrifugation at 13,000g for 10 min. GUS activity was measured with 1 mM 4-methylumbelliferyl β -D-glucuronide and 20% methanol.

Cloning, Expression, and Purification of the Recombinant Protein

The HB1 HD-Zip I region (amino acids 1 to 142) was expressed in pGEX-3X (GE Healthcare; Kaelin et al., 1992) using oligonucleotides HB1-HD-ZipF, 5'-GGGGATCCTCGGAATATAGCCAATA-3', and HB1-HD-ZipR, 5'-GGGGAATTCCTGTGAACACTACTGACTTTGC-3'. *Escherichia coli* cells, strain JM109 (GE Healthcare) transformed with the HB1 pGEX-3X fusions or the empty vector, were grown and induced as described (Palena et al., 1998). Recombinant proteins were purified using the glutathione S-transferase tag (GE Healthcare; Kaelin et al., 1992).

DNA Binding Assays

For electrophoretic mobility shift assays, 20 ng of purified recombinant protein were incubated with 0.5 ng of DNA generated by hybridization of the complementary synthetic oligonucleotides 5'-GATCCTTA(CENTRAL CORE)ATATGCG-3' and 5'-AATTCGCATAT(CENTRAL CORE)TAAG-3' and labeled with [α -³²P]dATP using the Klenow DNA polymerase (Promega). Derivative modified oligonucleotides were used in competition assays (20-fold excess). Binding reactions were performed as previously described (Palena et al., 1998). For competition, oligonucleotides used had the following central cores: in Figures 5A and 5B, (2) CAAT(A/T)ATTG, (3) CAAT(C/G)ATTG, (4) TAAT(A/T)ATTA, (5) CAGT(A/T)ACTG, (6) CATT(A/T)AATG, (7) CAAA(A/T)TTTG, (8) CAAC(A/T)GTTG, (9) CGAT(A/T)ATCG, and (10) CAGT(G/C)ACTG; and in Figure 5C, CAAT(A/T)ATTG, CAAT(C/G)ATTG and CAGGATCCG/CGGATCCTG.

ChIP-PCR Assays

The *ProMt HB1:HB1:2xFLAG:2xHA* construct was obtained using the MultiSite Gateway Cloning System (Invitrogen) and the destination vector pK7m34GW (Karimi et al., 2002). Transgenic roots bearing this construct were obtained. For each condition, 2 g of root tissues from composite plants were used for ChIP assays with α -HA antibodies (μ MACS; Miltenyi Biotec). Nuclei were isolated as described previously (Delaney et al., 2006). Purified nuclei were fixed with 1% formaldehyde for 20 min immediately after extraction. The immunoprecipitation of purified chromatin was performed using a ChIP assay kit (Millipore) according to the manufacturer's instructions, replacing the antibodies recognition and washing steps by the μ MACS antibodies and Separation Columns (Miltenyi Biotec) essentially as described by Hirsch et al. (2009).

Primers used for amplification of ChIP samples were LBDChF, 5'-CATTGAAGGGACACAGAATAC-3', and LBDChR, 5'-TGGACCCAT-TATAACCCAG-3'.

Bioinformatic Analyses

Related LBDs from *M. truncatula* were identified by BLAST (<http://www.ncbi.nlm.nih.gov/BLAST/>). The best-fit model of protein evolution was searched out using ProtTest (Abascal et al., 2005), which selected the WAG matrix plus G (gamma) and F (frequencies) modifiers for the whole sequences. The phylogenetic reconstruction was performed using the Bayesian inference algorithm implemented by the MrBayes 3 package (Huelsenbeck et al., 2001), including all of the identified *M. truncatula* LBD proteins, all of the *Arabidopsis thaliana* Class II LBDs, and a similar number of *Arabidopsis* Class I LBDs. The protein alignment of Mt HB1, At HB7, and At HB12 was performed by MAFFT 6.0 (Katoh and Toh, 2008) using the visualizing tool MView (Brown et al., 1998). The same colors indicate common chemical properties among the amino acids. To scan the promoter regions to search for the HD-Zip binding core, the REMORA Workflow GetAndScanPromoterRegionsFromAListOfMedicagoIDsTo-UniquelDs (http://lipm-bioinfo.toulouse.inra.fr/remora/cgi/configure.cgi?session_dir=18662642425344andform=fromfawandcomplete_workflow=1) from <http://www.legoo.org/> (Carrere and Gouzy, 2006) was used, with the TIGR TC ID list of genes differentially regulated in response to salt in root apices as query (Gruber et al., 2009). For the workflow configuration, the following parameters were set: promoter length, 2000 bp; PatScan strings were based on the box CAATNATTG, where N was replaced by A, C, G, and T in each submission, followed by [0,0,0], meaning that no mismatches, insertions, or deletions were allowed.

Accession Numbers

Sequence data from this article can be found in the Arabidopsis Genome Initiative or GenBank/EMBL databases under the following accession numbers: *M. truncatula* (MtGI9) *HB1* (or *HD1374*), TC117282; *LBD1*, TC121747; *ACT*, TC106786; *H3I*, TC117750; *RBP*, TC113147; *Arabidopsis HB7*, AT5G46880.1; and *HB12*, AT3G61890.1.

Supplemental Data

The following materials are available in the online version of this article.

Supplemental Figure 1. Effect of Different NaCl Concentrations on *M. truncatula* Root Architecture.

Supplemental Figure 2. Nodule Densities of *hb1-1* and Wild-Type Plants.

Supplemental Figure 3. Global Root Architecture and Microscopy Analysis of *hb1*, the Wild Type, and *35S:HB1* Plants in Control and Salt Stress Conditions.

Supplemental Figure 4. Histological Analysis of *hb1* Roots under Control and Salt Stress Conditions.

Supplemental Figure 5. Sequence Specificity of in Vitro DNA Recognition by the Recombinant HB1 DNA Binding Domain.

Supplemental Figure 6. Expression of HB1 Candidate Target Genes in *HB1* Overexpressing Roots.

Supplemental Figure 7. *ProHB1:GUS* Activity in Root Apices, Nodules, and Roots under Salt Stress or Treated with ABA.

Supplemental Figure 8. Fluorometric Analysis of *ProLBD1:GUS* and *Pro-MUT-LBD1:GUS* Activity in Response to ABA and IAA.

Supplemental Figure 9. Phylogenetic Tree of *Arabidopsis* and *M. truncatula* LBD Proteins.

Supplemental Table 1. List of Potential HB1 Direct Targets.

Supplemental Table 2. Mean Values, Standard Deviations, and Statistic Analyses of the Values Shown in All Figures.

Supplemental Data Set 1. Text File of the Alignment Corresponding to Supplemental Figure 9.

ACKNOWLEDGMENTS

We thank Adnane Boualem (Unité de Recherche en Génomique Végétale-Institut National de la Recherche Agronomique, Evry, France) for initial experiments on the effect of salt stress on *M. truncatula* root architecture, Phil Mullineaux (University of Essex, UK) and Alexis Maizel (Institut des Sciences du Végétal, Centre National de la Recherche Scientifique) for careful reading of the manuscript, and Jorge Giacomelli (IAL-CONICET, Argentina) for help with the phylogenetic analyses. We also thank the ECOS-Sud Project A07B03, the Saint-Exupéry program (French Embassy/Argentine Education Ministry), and the “Nuevo Banco Sta. Fe” Foundation for providing short-term fellowships to F.A. We also acknowledge the contributions of R. Thompson at Institut National de la Recherche Agronomique, Dijon, France, and J. Clarke for generating the TILLING resource at the John Innes Centre, Norwich, UK. The work in Argentina was supported by Agencia Nacional de Promoción Científica y Tecnológica (PICT 2005 38103 and PICT 2007 37000/022). R.C. is a member of CONICET, and F.A. is a fellow of the same institution. The support of the “Grain Legumes” FP6 EEC project (FOOD-CT-2004-506223) is also acknowledged.

Received February 18, 2010; revised May 31, 2010; accepted July 15, 2010; published July 30, 2010.

REFERENCES

- Abascal, F., Zardoya, R., and Posada, D. (2005). ProtTest: Selection of best-fit models of protein evolution. *Bioinformatics* **21**: 2104–2105.
- Ariel, F.D., Manavella, P.A., Dezar, C.A., and Chan, R.L. (2007). The true story of the HD-Zip family. *Trends Plant Sci.* **12**: 419–426.
- Boisson-Dernier, A., Chabaud, M., Garcia, F., Becard, G., Rosenberg, C., and Barker, D.G. (2001). *Agrobacterium rhizogenes*-transformed roots of *Medicago truncatula* for the study of nitrogen-fixing and endomycorrhizal symbiotic associations. *Mol. Plant Microbe Interact.* **14**: 695–700.
- Brady, S.M., Sarkar, S.F., Bonetta, D., and McCourt, P. (2003). The ABSCISIC ACID INSENSITIVE 3 (ABI3) gene is modulated by farnesylation and is involved in auxin signaling and lateral root development in *Arabidopsis*. *Plant J.* **34**: 67–75.
- Bright, L.J., Liang, Y., Mitchell, D.M., and Harris, J.M. (2005). The LATD gene of *Medicago truncatula* is required for both nodule and root development. *Mol. Plant Microbe Interact.* **18**: 521–532.
- Brown, N.P., Leroy, C., and Sander, C. (1998). MView: A web-compatible database search or multiple alignment viewer. *Bioinformatics* **14**: 380–381.
- Cannon, S.B., May, G.D., and Jackson, S.A. (2009). Three sequenced legume genomes and many crop species: Rich opportunities for translational genomics. *Plant Physiol.* **151**: 970–977.
- Carrere, S., and Gouzy, J. (2006). REMORA: A pilot in the ocean of BioMoby web-services. *Bioinformatics* **22**: 900–901.
- Choi, H.-K., Mun, J.-H., Kim, D.-J., Zhu, H., Baek, J.-M., Mudge, J., Roe, B., Ellis, N., Doyle, J., Kiss, G.B., Young, N.D., and Cook, D.R. (2004). Estimating genome conservation between crop and model legume species. *Proc. Natl. Acad. Sci. USA* **101**: 15289–15294.
- Crespi, M., and Frugier, F. (2008). De novo organ formation from differentiated cells: Root nodule organogenesis. *Sci. Signal.* **1**: re11.
- Delaney, K.J., Xu, R., Zhang, J., Li, Q.Q., Yun, K.Y., Falcone, D.L., and Hunt, A.G. (2006). Calmodulin interacts with and regulates the RNA-binding activity of an *Arabidopsis* polyadenylation factor subunit. *Plant Physiol.* **140**: 1507–1521.
- de Lorenzo, L., Merchan, F., Laporte, P., Thompson, R., Clarke, J., Sousa, C., and Crespi, M. (2009). A novel plant leucine-rich repeat receptor kinase regulates the response of *Medicago truncatula* roots to salt stress. *Plant Cell* **21**: 668–680.
- De Smet, I., Signora, L., Beeckman, T., Inze, D., Foyer, C.H., and Zhang, H. (2003). An abscisic acid-sensitive checkpoint in lateral root development of *Arabidopsis*. *Plant J.* **33**: 543–555.
- De Smet, I., Zhang, H., Inze, D., and Beeckman, T. (2006). A novel role for abscisic acid emerges from underground. *Trends Plant Sci.* **11**: 434–439.
- Dezar, C.A., Fedrigo, G.V., and Chan, R.L. (2005). The promoter of the sunflower HD-Zip protein gene Hahb4 directs tissue-specific expression and is inducible by water stress, high salt concentrations and ABA. *Plant Sci.* **169**: 447–459.
- Ding, Y., Kalo, P., Yendrek, C., Sun, J., Liang, Y., Marsh, J.F., Harris, J.M., and Oldroyd, G.E.D. (2008). Abscisic acid coordinates Nod factor and cytokinin signaling during the regulation of nodulation in *Medicago truncatula*. *Plant Cell* **20**: 2681–2695.
- Dubrovsky, J.G., Sauer, M., Napsucially-Mendivil, S., Ivanchenko, M.G., Friml, J., Shishkova, S., Celenza, J., and Benková, E. (2008). Auxin acts as a local morphogenetic trigger to specify lateral root founder cells. *Proc. Natl. Acad. Sci. USA* **105**: 8790–8794.
- Fukaki, H., and Tasaka, M. (2009). Hormone interactions during lateral root formation. *Plant Mol. Biol.* **69**: 437–449.
- Georgin, P., and Gouet, M. (2000). Statistiques avec Excell. (Paris: Eyrolles).
- Gonzalez-Rizzo, S., Crespi, M., and Frugier, F. (2006). The *Medicago truncatula* CRE1 cytokinin receptor regulates lateral root development and early symbiotic interaction with *Sinorhizobium meliloti*. *Plant Cell* **18**: 2680–2693.
- Gruber, V., Blanchet, S., Diet, A., Zahaf, O., Boualem, A., Kakar, K., Alunni, B., Udvardi, M., Frugier, F., and Crespi, M. (2009). Identification of transcription factors involved in root apex responses to salt stress in *Medicago truncatula*. *Mol. Genet. Genomics* **281**: 55–66.
- Hirsch, S., Kim, J., Muñoz, A., Heckmann, A.B., Downie, A., and Oldroyd, G. (2009). GRAS proteins form a DNA binding complex to induce gene expression during nodulation signaling in *Medicago truncatula*. *Plant Cell* **21**: 545–557.
- Henriksson, E., Olsson, A.S.B., Johannesson, H., Johansson, H., Hanson, J., Engstrom, P., and Soderman, E. (2005). Homeodomain Leucine Zipper Class I genes in *Arabidopsis*. Expression patterns and phylogenetic relationships. *Plant Physiol.* **139**: 509–518.
- Hochholdinger, F., and Zimmermann, R. (2008). Conserved and diverse mechanisms in root development. *Curr. Opin. Plant Biol.* **11**: 70–74.

- Hofer, J., Turner, L., Moreau, C., Ambrose, M., Isaac, P., Butcher, S., Weller, J., Dupin, A., Dalmais, M., Le Signor, C., Bendahmane, A., and Ellis, N. (2009). Tendril-less regulates tendril formation in pea leaves. *Plant Cell* **21**: 420–428.
- Huelsensbeck, J.P., Ronquist, F., Nielsen, R., and Bollback, J.P. (2001). Bayesian inference of phylogeny and its impact on evolutionary biology. *Science* **294**: 2310–2314.
- Husbands, A., Bell, E.M., Shuai, B., Smith, H.M.S., and Springer, P.S. (2007). LATERAL ORGAN BOUNDARIES defines a new family of DNA-binding transcription factors and can interact with specific bHLH proteins. *Nucleic Acids Res.* **35**: 6663–6671.
- Kaelin, W.G., Krek, W., Sellers, W.R., DeCaprio, J.A., Ajchenbaum, F., Fuchs, C.S., Chittenden, T., Li, Y., Farnham, P.J., and Blar, M.A. (1992). Expression cloning of a cDNA encoding a retinoblastoma-binding protein with E2F-like properties. *Cell* **70**: 351–364.
- Karimi, M., Inze, D., and Depicker, A. (2002). GATEWAY vectors for *Agrobacterium*-mediated plant transformation. *Trends Plant Sci.* **7**: 193–195.
- Katoh, K., and Toh, H. (2008). Recent developments in the MAFFT multiple sequence alignment program. *Brief. Bioinform.* **9**: 286–298.
- Lee, H.W., Kim, N.Y., Lee, D.J., and Kim, J. (2009). LBD18/ASL20 regulates lateral root formation in combination with LBD16/ASL18 downstream of ARF7 and ARF19 in *Arabidopsis*. *Plant Physiol.* **151**: 1377–1389.
- Le Signor, C., Savoie, V., Aubert, G., Verdier, J., Nicolas, M., Pagny, G., Moussy, F., Sanchez, M., Baker, D., Clarke, J., and Thompson, R. (2009). Optimizing TILLING populations for reverse genetics in *Medicago truncatula*. *Plant Biotechnol. J.* **7**: 430–441.
- Liang, Y., and Harris, J.M. (2005). Response of root branching to abscisic acid is correlated with nodule formation both in legumes and non-legumes. *Am. J. Bot.* **92**: 1675–1683.
- Liang, Y., Mitchell, D.M., and Harris, J.M. (2007). Abscisic acid rescues the root meristem defects of the *Medicago truncatula latd* mutant. *Dev. Biol.* **304**: 297–307.
- Liu, H., Wang, S., Yu, X., Yu, J., He, X., Zhang, S., Shou, H., and Wu, P. (2005). ARL1, a LOB-domain protein required for adventitious root formation in rice. *Plant J.* **43**: 47–56.
- Malamy, J.E., and Benfey, P.N. (1997). Organization and cell differentiation in lateral roots of *Arabidopsis thaliana*. *Development* **124**: 33–44.
- Manavella, P.A., Dezar, C.A., Ariel, F.D., and Chan, R.L. (2008). Two ABREs, two redundant root-specific and one W-box cis-acting elements are functional in the sunflower HAHB4 promoter. *Plant Physiol. Biochem.* **46**: 860–867.
- Merchan, F., de Lorenzo, L., Rizzo, S.G., Niebel, A., Manyani, H., Frugier, F., Sousa, C., and Crespi, M. (2007). Identification of regulatory pathways involved in the reacquisition of root growth after salt stress in *Medicago truncatula*. *Plant J.* **51**: 1–17.
- Okushima, Y., et al. (2005). Functional genomic analysis of the AUXIN RESPONSE FACTOR gene family members in *Arabidopsis thaliana*: Unique and overlapping functions of ARF7 and ARF19. *Plant Cell* **17**: 444–463.
- Olsson, A.S., Engstrom, P., and Soderman, E. (2004). The homeobox genes ATHB12 and ATHB7 encode potential regulators of growth in response to water deficit in *Arabidopsis*. *Plant Mol. Biol.* **55**: 663–677.
- Osmont, K.S., Sibout, R., and Hardtke, C.S. (2007). Hidden branches: Developments in root system architecture. *Annu. Rev. Plant Biol.* **58**: 93–113.
- Palena, C.M., Gonzalez, D.H., Guelman, S.A., and Chan, R.L. (1998). Expression of sunflower homeodomain containing proteins in *Escherichia coli*: Purification and functional studies. *Protein Expr. Purif.* **13**: 97–103.
- Penmetza, R.V., et al. (2008). The *Medicago truncatula* ortholog of *Arabidopsis* EIN2, *sickle*, is a negative regulator of symbiotic and pathogenic microbial associations. *Plant J.* **55**: 580–595.
- Peret, B., De Rybel, B., Casimiro, I., Benkova, E., Swarup, R., Laplaze, L., Beekman, T., and Bennett, M.J. (2009b). *Arabidopsis* lateral root development: An emerging story. *Trends Plant Sci.* **14**: 399–408.
- Peret, B., Larrieu, A., and Bennett, M.J. (2009a). Lateral root emergence: A difficult birth. *J. Exp. Bot.* **60**: 3637–3643.
- Perez-Torres, C.-A., Lopez-Bucio, J., Cruz-Ramirez, A., Ibarra-Laclette, E., Dharmasiri, S., Estelle, M., and Herrera-Estrella, L. (2008). Phosphate availability alters lateral root development in *Arabidopsis* by modulating auxin sensitivity via a mechanism involving the TIR1 auxin receptor. *Plant Cell* **20**: 3258–3272.
- Rubin, G., Tohge, T., Matsuda, F., Saito, K., and Scheible, W.-R. (2009). Members of the LBD family of transcription factors repress anthocyanin synthesis and affect additional nitrogen responses in *Arabidopsis*. *Plant Cell* **21**: 3567–3584.
- Shuai, B., Reynaga-Pena, C.G., and Springer, P.S. (2002). The LATERAL ORGAN BOUNDARIES gene defines a novel, plant-specific gene family. *Plant Physiol.* **129**: 747–761.
- Signora, L., De Smet, I., Foyer, C.H., and Zhang, H. (2001). ABA plays a central role in mediating the regulatory effects of nitrate on root branching in *Arabidopsis*. *Plant J.* **6**: 655–662.
- Soderman, E., Mattsson, J., and Engstrom, P. (1996). The *Arabidopsis* homeobox gene ATHB-7 is induced by water deficit and by abscisic acid. *Plant J.* **10**: 375–381.
- Soderman, E., Mattsson, J., Svenson, M., Borkird, C., and Engstrom, P. (1994). Expression patterns of novel genes encoding homeodomain leucine-zipper proteins in *Arabidopsis thaliana*. *Plant Mol. Biol.* **26**: 145–154.
- Swarup, K., et al. (2008). The auxin influx carrier LAX3 promotes lateral root emergence. *Nat. Cell Biol.* **10**: 946–954.
- Truchet, G., Debelle, F., Vasse, J., Terzaghi, B., Garnerone, A.M., Rosenberg, C., Batut, J., Maillet, F., and Denarie, J. (1985). Identification of a *Rhizobium meliloti* pSym2011 region controlling the host specificity of root hair curling and nodulation. *J. Bacteriol.* **164**: 1200–1210.
- Udvardi, M.K., Kakar, K., Wandrey, M., Montanari, O., Murray, J., Andriankaja, A., Zhang, J.-Y., Benedito, V., Hofer, J.M.I., Chueng, F., and Town, C.D. (2007). Legume transcription factors: Global regulators of plant development and response to the environment. *Plant Physiol.* **144**: 538–549.
- Vandesompele, J., De Preter, K., Pattyn, F., Poppe, B., Van Roy, N., De Paepe, A., and Speleman, F. (2002). Accurate normalization of real-time quantitative RT-PCR data by geometric averaging of multi-internal control genes. *Genome Biol.* **3**: RESEARCH0034.
- Welchen, E., and Gonzalez, D.H. (2005). Differential expression of the *Arabidopsis* cytochrome *c* genes *Cytc-1* and *Cytc-2*: Evidence for the involvement of TCP-domain protein binding elements in anther and meristem-specific expression of the *Cytc-1* gene. *Plant Physiol.* **139**: 88–100.
- Wolters, H., and Jurgens, G. (2009). Survival of the flexible: Hormonal growth control and adaptation in plant development. *Nat. Rev. Genet.* **10**: 305–317.
- Wopereis, J., Pajuelo, E., Dazzo, F.B., Jiang, Q., Gresshoff, P.M., De Bruijn, F.J., Stougaard, J., and Szczyglowski, K. (2000). Short root mutant of *Lotus japonicus* with a dramatically altered symbiotic phenotype. *Plant J.* **23**: 97–114.
- Xiong, L., Wang, R.G., Mao, G., and Koczan, J.M. (2006). Identification of drought tolerance determinants by genetic analysis of root response to drought stress and abscisic acid. *Plant Physiol.* **142**: 1065–1074.
- Yendrek, C.R., et al. (2010). A putative transporter is essential for integrating nutrient and hormone signaling with lateral root growth and nodule development in *Medicago truncatula*. *Plant J.* **62**: 100–112.

Environmental Regulation of Lateral Root Emergence in *Medicago truncatula* Requires the HD-Zip I Transcription Factor HB1

Federico Ariel, Anouck Diet, Verdenaud Marion, Véronique Gruber, Frugier Florian, Raquel Chan and Martin Crespi

PLANT CELL published online Jul 30, 2010;
DOI: 10.1105/tpc.110.074823

This information is current as of July 30, 2010

Supplemental Data	http://www.plantcell.org/cgi/content/full/tpc.110.074823/DC1
Permissions	https://www.copyright.com/ccc/openurl.do?sid=pd_hw1532298X&issn=1532298X&WT.mc_id=pd_hw1532298X
eTOCs	Sign up for eTOCs for <i>THE PLANT CELL</i> at: http://www.plantcell.org/subscriptions/etoc.shtml
CiteTrack Alerts	Sign up for CiteTrack Alerts for <i>Plant Cell</i> at: http://www.plantcell.org/cgi/alerts/ctmain
Subscription Information	Subscription information for <i>The Plant Cell</i> and <i>Plant Physiology</i> is available at: http://www.aspb.org/publications/subscriptions.cfm